

Studies on Enantioselective Liquid–Liquid Extraction of Amino-(4-nitro-phenyl)-acetic Acid Enantiomers: Modeling and Optimization

PANLIANG ZHANG,¹ CHANG LIU,² KEWEN TANG,^{1*} JIAJIA LIU,² CONGSHAN ZHOU,¹ AND CHANGAN YANG¹

¹Department of Chemistry and Chemical Engineering, Hunan Institute of Science and Technology, Hunan, China

²College of Chemistry and Chemical Engineering, Central South University, Hunan, China

ABSTRACT BINAP-metal complexes were prepared as extractant for enantioselective liquid–liquid extraction (ELLE) of amino-(4-nitro-phenyl)-acetic acid (NPA) enantiomers. The influence of process variables, including types of organic solvents and metal precursor, concentration of ligand, pH, and temperature on the efficiency of the extraction, were investigated experimentally. An interfacial reaction model was established for insightful understanding of the chiral extraction process. Important parameters required for the model were determined. The experimental data were compared with model predictions to verify the model prediction, it was found that the interfacial reaction model predicted the experimental results accurately. By modeling and experiment, an optimal extraction condition with pH of 7 and host (extractant) concentration of 1 mmol/L was obtained and high enantioselectivity (α_{op}) of 3.86 and performance factor (β) of 0.1949 were achieved. *Chirality* 26:79–87, 2014. © 2013 Wiley Periodicals, Inc.

KEY WORDS: enantioselective liquid-liquid extraction; BINAP; metal complex; enantiomers; model

INTRODUCTION

The production and availability of enantiomerically pure compounds is of prime importance to the pharmaceutical industry as well as to the agrochemical, flavor, and fragrance industries.^{1–3} The most common technique for obtaining enantiomerically pure compounds on a commercial scale is classical resolution by crystallization but the method has low versatility.⁴ Compared with crystallization and some other methods, such as chiral liquid chromatography⁵ and chiral capillary electrophoresis,⁶ enantioselective liquid–liquid extraction (ELLE) is expected to be cheaper and easier to scale up to commercial scale and has a large application range.^{7,8}

A chiral selector plays an important role in ELLE, which binds enantiospecifically and reversibly with a racemic substrate.⁹ Several chiral selectors have been reported, such as tartaric acid derivatives,^{10,11} crown ethers,^{12–14} cinchona alkaloids,^{9,15} β -CD derivatives,^{16–19} metal complex,²⁰ and so on^{21–27}. The chiral bisphosphine BINAP, which has been proven to be a highly versatile ligand in asymmetric catalysis, makes it possible to bind other ligands by exchange of a counterion. Therefore, the BINAP–metal complex may provide an efficient selector in ELLE. Some interesting examples can be found in previous work for ELLE of amino acid enantiomers.^{28,29}

Amino acid enantiomers are increasingly important to industrial and laboratory processes, as they are considered crucial chiral building blocks for a variety of biologically active compounds, such as pesticides, peptides, and semisynthetic β -lactam antibiotics. Amino-(4-nitro-phenyl)-acetic acid (NPA) can be used as a D-serine transporter inhibitor for the treatment of nervous system disorders.³⁰ It can be seen as adding a nitro to para-position of phenylglycine (Fig. 1).

This paper reports the ELLE of NPA enantiomers with (S)-BINAP metal complex as the chiral extractant. The factors affecting the extraction efficiency, such as types of metal ions and organic solvents, pH of aqueous phase, concentrations of host, and temperature, were investigated. The equilibrium of the extraction system was modeled and optimized by an interfacial reaction model.

© 2013 Wiley Periodicals, Inc.

THEORY AND MODELING

Theory of Enantioselective Reactive Extraction

Knowledge of the reaction mechanism is required to gain a better understanding of the reactive extraction process. Two different mechanisms have been reported in previous works on reactive extraction, namely, homogeneous ligand addition mechanism and interfacial ligand exchange mechanism. The main difference between the two mechanisms is the locus of the complexation reaction.

In enantioselective extraction of NPA enantiomers by CuPF₆ {(S)-BINAP} (the extractant, written as BINAP-Cu for short), the reaction between NPA enantiomers and the extractant occurs either in one of the phases or at the interface. It was found that the metal–BINAP complex is highly hydrophobic, which excludes the possibility that the complexation reaction takes place in the aqueous phase. The complexation reaction could only happen either in the organic phase or at the interface. Where the complexation reaction occurs depends on the solubility of the reactant and the product of the complexation reaction. It was found that NPA enantiomers could distribute over the organic and aqueous phases. NPA anion can react with BINAP-Cu through a ligand-exchange process. One mol of NPA reacts with 1 mol of BINAP-Cu and generates 1 mol of PF₆. Although NPA enantiomers and BINAP-Cu can exist in the organic phase, the product of this reaction PF₆ can hardly exist in the organic phase (Fig. 2). It is concluded that the

Contract grant sponsor: National Science Foundation of China; Contract grant number: 21171054.

Contract grant sponsor: Open Fund Project of Key Laboratory in Hunan University; Contract grant number: 11K029.

Contract grant sponsor: Key Laboratory of Hunan Province.

Contract grant sponsor: Aid Program for Science and Technology Innovative Research Team in Higher Educational Institutions of Hunan Province.

*Correspondence to: Kewen Tang, Department of Chemistry and Chemical Engineering, Hunan Institute of Science and Technology, Yueyang 414006, Hunan, China. E-mail: tangkewen@sina.com

Received for publication 2 August 2013; Accepted 8 October 2013

DOI: 10.1002/chir.22266

Published online 10 December 2013 in Wiley Online Library (wileyonlinelibrary.com).

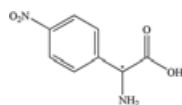


Fig. 1. Chemical structure of NPA.

reaction takes place at the interface between the two phases. Therefore, the interfacial ligand exchange mechanism was applied in this paper for studying the reactive extraction of NPA enantiomers by BINAP-Cu.

Model Equations

Consider the volume of aqueous phase (V_w) equal to the volume of organic phase (V_{org}). Species in both phases are in chemical equilibrium, and each phase is open with respect to the other. The enantioselective reactive liquid-liquid extraction system can be modeled by a series of coupled equilibrium relations and mass balance equations as follows.

The acid dissociation equilibrium constant in aqueous phase:

$$K_a = \frac{[H^+][D^-]_w}{[DH]_w} = \frac{[H^+][L^-]_w}{[LH]_w} \quad (1)$$

where $[DH]_w$ and $[LH]_w$ are the concentrations of the molecular D- and L-NPA in the aqueous phase at equilibrium, respectively; $[D^-]_w$ and $[L^-]_w$ are the concentrations of the D- and L-NPA anion in the aqueous phase at equilibrium, respectively.

The physical partition coefficient of molecular D- and L-NPA, P_0 , can be written as follows:

$$P_0 = \frac{[DH]_{org}}{[DH]_w} = \frac{[LH]_{org}}{[LH]_w} \quad (2)$$

and the physical partition coefficient of the D- and L-NPA anion, P_i , can be written as follows:

$$P_i = \frac{[D^-]_{org}}{[D^-]_w} = \frac{[L^-]_{org}}{[L^-]_w} \quad (3)$$

where $[DH]_{org}$ and $[LH]_{org}$ are the concentrations of the molecular D- and L-NPA in the organic phase at equilibrium,

respectively; $[D^-]_{org}$ and $[L^-]_{org}$ are the concentrations of the D- and L-NPA anion in the organic phase at equilibrium, respectively.

The complexation equilibrium of BINAP-Cu with NPA enantiomers at the interface can be written as follows:

$$K_D = \frac{[DCuB]_{org}[PF_6^-]_w}{[CuB]_{org}[D^-]_w} \quad (4)$$

$$K_L = \frac{[LCuB]_{org}[PF_6^-]_w}{[CuB]_{org}[L^-]_w} \quad (5)$$

where $[DCuB]_{org}$ and $[LCuB]_{org}$ are the concentrations of the complexes of BINAP-Cu with D- and L-NPA in the organic phase; $[CuB]_{org}$ is the concentration of BINAP-Cu in the organic phase at equilibrium; $[PF_6^-]_w$ is the concentration of PF_6^- in the aqueous phase.

Due to $V_w = V_{org}$, the following equations represent the mass balance for D- and L-NPA:

$$C_D = [DH]_w + [D^-]_w + [DH]_{org} + [D^-]_{org} + [DCuB]_{org} \quad (6)$$

$$C_L = [LH]_w + [L^-]_w + [LH]_{org} + [L^-]_{org} + [LCuB]_{org} \quad (7)$$

where C_D and C_L are the total concentrations of D- and L-NPA in the aqueous and organic phases.

Combining eqs. 1-5, eqs. 6 and 7 are deduced to:

$$C_D = \frac{[H^+][D^-]_w}{K_a} + [D^-]_w + \frac{P_0[H^+][D^-]_w}{K_a} + P_i[D^-]_w + \frac{K_D[D^-]_w[CuB]_{org}}{[PF_6^-]} \quad (8)$$

$$C_L = \frac{[H^+][L^-]_w}{K_a} + [L^-]_w + \frac{P_0[H^+][L^-]_w}{K_a} + P_i[L^-]_w + \frac{K_L[L^-]_w[CuB]_{org}}{[PF_6^-]} \quad (9)$$

There is the following equation for mass balance of BINAP-Cu complex:

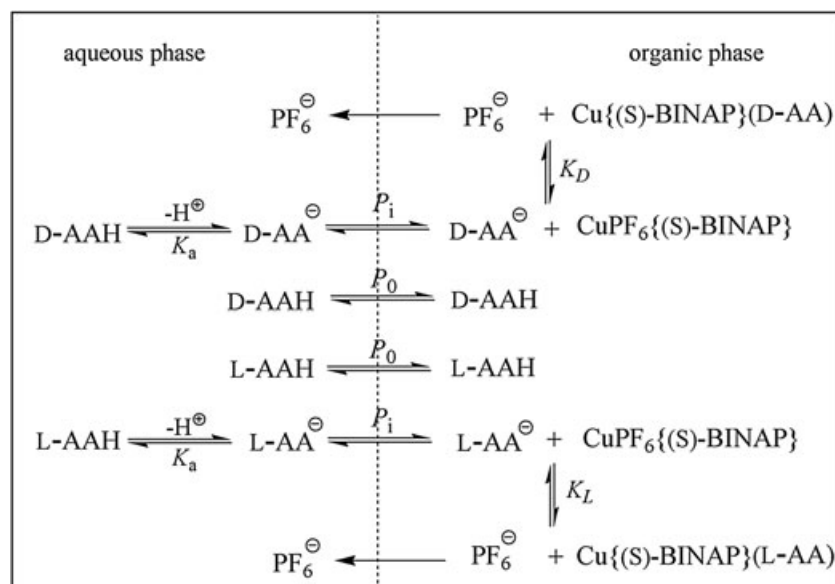


Fig. 2. Diagram of enantioselective extraction of NPA enantiomers.

$$C_{\text{CuB}} = [\text{CuB}]_{\text{org}} + [\text{DCuB}]_{\text{org}} + [\text{LCuB}]_{\text{org}} \quad (10)$$

where C_{CuB} is the initial concentration of BINAP-Cu.

Combining eqs. 4 and 5, eq. 10 is deduced to

$$C_{\text{CuB}} = [\text{CuB}]_{\text{org}} + \frac{K_{\text{D}}[\text{D}^-]_{\text{w}}[\text{CuB}]_{\text{org}}}{[\text{PF}_6^-]_{\text{w}}} + \frac{K_{\text{L}}[\text{L}^-]_{\text{w}}[\text{CuB}]_{\text{org}}}{[\text{PF}_6^-]_{\text{w}}} \quad (11)$$

Let $A = \frac{[\text{H}^+]}{K_{\text{a}}} + 1 + \frac{P_0[\text{H}^+]}{K_{\text{a}}} + P_i$ and combine eqs. 8, 9, and 10, the following equation is obtained,

$$C_{\text{CuB}} = [\text{CuB}]_{\text{org}} + \frac{K_{\text{D}}C_{\text{D}}[\text{CuB}]_{\text{org}}}{A(C_{\text{CuB}} - [\text{CuB}]_{\text{org}}) + K_{\text{D}}[\text{CuB}]_{\text{org}}} + \frac{K_{\text{L}}C_{\text{L}}[\text{CuB}]_{\text{org}}}{A(C_{\text{CuB}} - [\text{CuB}]_{\text{org}}) + K_{\text{L}}[\text{CuB}]_{\text{org}}} \quad (12)$$

With a further treatment of eq. 12, the following equation can be deduced:

$$\begin{aligned} & (K_{\text{D}}K_{\text{L}} - K_{\text{D}}A - K_{\text{L}}A + A^2)[\text{CuB}]^3 \\ & + (2K_{\text{D}}AC_{\text{CuB}} + 2K_{\text{L}}AC_{\text{CuB}} - 3A^2C_{\text{CuB}} + K_{\text{D}}K_{\text{L}}C_{\text{D}} \\ & - K_{\text{D}}C_{\text{D}}A + K_{\text{D}}K_{\text{L}}C_{\text{L}} - K_{\text{L}}C_{\text{L}}A - K_{\text{D}}K_{\text{L}}C_{\text{CuB}})[\text{CuB}]^2 \\ & + (K_{\text{D}}C_{\text{D}}AC_{\text{CuB}} + K_{\text{L}}C_{\text{L}}AC_{\text{CuB}} - K_{\text{D}}AC_{\text{CuB}}^2 \\ & + K_{\text{L}}AC_{\text{CuB}}^2) + 3A^2C_{\text{CuB}}^2)[\text{CuB}] - A^2C_{\text{CuB}}^3 = 0 \end{aligned} \quad (13)$$

Since $[\text{CuB}]_{\text{org}}$ can be obtained by solving eq. 12, distribution ratios can be written as follows:

$$k_{\text{D}} = \frac{P_0[\text{H}^+] + P_iK_{\text{a}} + \frac{P_iK_{\text{D}}K_{\text{a}}[\text{CuB}]_{\text{org}}}{C_{\text{CuB}} - [\text{CuB}]_{\text{org}}}}{K_{\text{a}} + [\text{H}^+]} \quad (14)$$

$$k_{\text{L}} = \frac{P_0[\text{H}^+] + P_iK_{\text{a}} + \frac{P_iK_{\text{L}}K_{\text{a}}[\text{CuB}]_{\text{org}}}{C_{\text{CuB}} - [\text{CuB}]_{\text{org}}}}{K_{\text{a}} + [\text{H}^+]} \quad (15)$$

Enantioselectivity is defined as:

$$\alpha_{\text{op}} = \frac{k_{\text{L}}}{k_{\text{D}}} \quad (16)$$

$$\alpha_{\text{int}} = \frac{K_{\text{L}}}{K_{\text{D}}} \quad (17)$$

where α_{op} is the operational selectivity, α_{int} is the intrinsic selectivity.

A common alternative measure of system performance is provided by the enantiomeric excess (ee), which can be expressed in terms of distribution ratios by the following equation:

$$ee_{\text{org}} = \frac{\frac{C_{\text{L}}}{1+1/k_{\text{L}}} - \frac{C_{\text{D}}}{1+1/k_{\text{D}}}}{\frac{C_{\text{L}}}{1+1/k_{\text{L}}} + \frac{C_{\text{D}}}{1+1/k_{\text{D}}}} \quad (18)$$

The fraction of the solute i ($i = \text{D}$ or L) extracted into the aqueous phase (f_i) is given by

$$f_i = \frac{C_{i,\text{org}}}{C_i} \quad (19)$$

Where $C_{i,\text{org}}$ represents the total concentration of the solute i in organic phase at equilibrium, and C_i represents the initial total concentration of the solute i .

The extraction performance factor (pf) is a very useful tool to optimize an enantioselective extraction and is defined as:

$$pf_i = f_i ee_{\text{org}} \quad (20)$$

A performance factor close to unity indicated a high enantiomeric purity in both phases.

Regression of the Complexation Equilibrium Constants

Regression of the complexation equilibrium constants was carried out as follows. Combining eqs. 1^{–5}, 14 and 15, the following equation can be achieved (let $B = \frac{[\text{H}^+]}{K_{\text{a}}} + 1$):

$$\begin{aligned} & (Bk_{\text{D}} - P_0\frac{[\text{H}^+]}{K_{\text{a}}} - P_i)\left(\frac{C_{\text{D}}k_{\text{D}}}{k_{\text{D}} + 1} + \frac{C_{\text{L}}k_{\text{L}}}{k_{\text{L}} + 1}\right) \\ & - \frac{([\text{D}]_{\text{w},\text{total}} + [\text{L}]_{\text{w},\text{total}})(P_i + (B-1)P_0)}{B} \end{aligned} \quad (21)$$

$$= K_{\text{D}}\left(C_{\text{CuB}} - \frac{C_{\text{D}}k_{\text{D}}}{k_{\text{D}} + 1} - \frac{C_{\text{L}}k_{\text{L}}}{k_{\text{L}} + 1}\right) + \frac{([\text{D}]_{\text{w},\text{total}} + [\text{L}]_{\text{w},\text{total}})(P_i + (B-1)P_0)}{B}$$

$$\begin{aligned} & (Bk_{\text{L}} - P_0\frac{[\text{H}^+]}{K_{\text{a}}} - P_i)\left(\frac{C_{\text{D}}k_{\text{D}}}{k_{\text{D}} + 1} + \frac{C_{\text{L}}k_{\text{L}}}{k_{\text{L}} + 1}\right) \\ & - \frac{([\text{D}]_{\text{w},\text{total}} + [\text{L}]_{\text{w},\text{total}})(P_i + (B-1)P_0)}{B} \end{aligned} \quad (22)$$

$$= K_{\text{L}}\left(C_{\text{CuB}} - \frac{C_{\text{D}}k_{\text{D}}}{k_{\text{D}} + 1} - \frac{C_{\text{L}}k_{\text{L}}}{k_{\text{L}} + 1}\right) + \frac{([\text{D}]_{\text{w},\text{total}} + [\text{L}]_{\text{w},\text{total}})(P_i + (B-1)P_0)}{B}$$

where $[\text{D}]_{\text{w},\text{total}}$ and $[\text{L}]_{\text{w},\text{total}}$ are the total concentration of D- and L-NPA in the aqueous phase at equilibrium, respectively. By linear regression of the experimental data according to eqs. 21 and 22, the equilibrium constants, K_{D} and K_{L} are evaluated from the slop of the fitting lines.

MATERIALS AND METHODS

Materials

Bi(acetonitrile)dichloropalladium(II) ($\text{PdCl}_2(\text{CH}_3\text{CN})_2$, mass fraction >97%) was purchased from the Metallurgy Institute of Zhejiang (Zhejiang, China). Bis(triphenylphosphine)nickel(II) ($(\text{C}_6\text{H}_5)_3\text{P})_2\text{NiCl}_2$, mass fraction >98%) and tetrakis(acetonitrile)copper(I) hexafluorophosphate ($(\text{CH}_3\text{CN})_4\text{Cu}[\text{PF}_6]$, mass fraction >98%) were purchased from Hwei Chemical (Guangzhou, China). 2,2'-Bis(diphenylphosphino)-1,1'-binaphthalene (BINAP, mass fraction >99%) was purchased from Shengjia Chemical. Racemic NPA was purchased from HanHong Biochemical (Jiangsu, China). The chiral extractants (BINAP-metal complexes) used in this paper were generated in situ by adding the metal precursor and BINAP in equal molar amounts to the appropriate organic solvent. The reaction mixture was stirred overnight and diluted to the desired concentration and the resulting solution was directly applied in extraction experiments as the organic phase. Solvent for chromatography was of high-performance liquid chromatography (HPLC) grade. Purified water was obtained by reverse osmosis followed by distillation.

All other chemicals were of analytical-reagent grade and bought from different suppliers.

Determination of Physical Distribution Coefficients P_0 and P_i

Experiments to determine the physical distribution coefficients of molecular and ionic NPA (P_0 and P_i) over the aqueous phase and 1,2-dichloroethane were carried out in a water bath at 5 °C. The aqueous phase were prepared by dissolving 2.0 mmol/L NPA in 0.1 mol/L sodium phosphate buffer solutions with a series of pH values in the range 3~9. Equal volumes of the two phases (each 2 mL) were placed together and shaken sufficiently for 12 h before being kept in a water bath at 5 °C to reach equilibrium. The concentrations of NPA enantiomers in the aqueous phase were analyzed by HPLC. The concentrations of NPA enantiomers in the organic phase was calculated from a mass balance.

Determination of Complexation Equilibrium Constants K_D and K_L

Reactive extraction experiments were carried out to obtain the complexation equilibrium constants of BINAP-Cu with NPA enantiomers. The racemic NPA was dissolved in sodium phosphate buffer solution (phosphate concentration = 0.10 mol/L, pH = 7.0) with a concentration of 1.0 mmol/L. BINAP-Cu was dissolved in 1,2-dichloroethane with a changing concentration from 0.25 mmol/L to 2 mmol/L. The two phases were put together in a test tube with equal amounts (each 2 mL) and stirred for 12 h at 5 °C. After equilibrium, the composition of the aqueous phase was analyzed by HPLC.

Extraction Experiments

The aqueous phase was prepared by dissolving racemic NPA in 0.1 mol/L phosphate buffer solution, and the organic phase was prepared by dissolving equimolar amounts of the metal precursor ($\text{PdCl}_2(\text{CH}_3\text{CN})_2$, $[(\text{CH}_3\text{CN})_4\text{Cu}]\text{PF}_6$, $[(\text{C}_6\text{H}_5)_3\text{P}]\text{NiCl}_2$) and BINAP in the appropriate organic solvent and the solution was stirred overnight before being used. Equal volumes of host-containing organic phase and NPA-containing aqueous phase (each 2 mL) were added to a 10-mL centrifuge tube and shaken sufficiently for 12 h at a fixed temperature of 5 °C before being kept in a water bath at 5 °C for 12 h to reach equilibrium. Then the tube was centrifuged to accelerate phase separation and the organic phase was discarded. The aqueous phase was analyzed by HPLC to obtain the concentrations of NPA enantiomers in the aqueous phase. The concentrations of NPA enantiomers in the organic phase were calculated from a mass balance.

Analytical Method

The quantification of NPA enantiomers in the aqueous phase was performed by HPLC using a WATERS e2695 apparatus (Waters, Milford, MA). A UV detector operated at 260 nm was applied. The column was diamonsil C18, 5 μm particle size of the packing material, 250 \times 4.6 mm I.D. (Dikma Technologies, Beijing China). The mobile phase was a 1:4 (v/v) mixture of methanol and a 0.1 mol/L acid sodium phosphate solution containing 0.5 mmol/L of cupric sulfate and 2.0 mmol/L of L-phenylalanine at pH = 4.8 (pH was adjusted with acetic acid). The flow rate was set at 1 mL/min and the column temperature was set at 27 °C.

RESULTS AND DISCUSSION

Physical Distribution Coefficients P_0 and P_i

Physical distribution coefficients for molecular and ionic NPA (P_0 and P_i) were determined through a series of physical extraction (extraction without extractant in the organic phase) experiments mentioned above. The apparent partition coefficients P_{app} were determined at different pH values. As described in Figure 2, both the molecular and ionic NPA can distribute over the organic and aqueous phases.

Then P_{app} is given by

Chirality DOI 10.1002/chir

$$P_{app} = \frac{[\text{AH}]_{org} + [\text{A}^-]_{org}}{[\text{AH}]_w + [\text{A}^-]_w} \quad (23)$$

where $[\text{AH}]_{org}$ and $[\text{A}^-]_{org}$ are the equilibrium concentrations of the molecular and ionic NPA in the organic phase, respectively; $[\text{AH}]_w$ and $[\text{A}^-]_w$ are the equilibrium concentrations of the molecular and ionic NPA in the aqueous phase, respectively.

Combining eqs. 1–3, eq. 23 can be derived as:

$$P_{app} \left(1 + \frac{[\text{H}^+]}{K_a} \right) = P_0 \frac{[\text{H}^+]}{K_a} + P_i \quad (24)$$

The pK_a of 5.60 was determined by potentiometric titration. The plot of $P_{app}(1 + [\text{H}^+]/K_a)$ versus $[\text{H}^+]/K_a$ yielded a straight line (in Fig. 3). The slope and intercept of the line were used to evaluate P_0 as 0.01074 and P_i as 0.08095, respectively.

Complexation Equilibrium Constants K_D and K_L

Complexation equilibrium constants could be determined through a series of reactive extraction experiments described in the experimental section. Figure 4 shows the regression analysis of the experimental data according to eqs. 21 and 22. We defined parameter $X = (C_{\text{CuB}} \frac{C_D k_D}{k_D+1} \frac{C_L k_L}{k_L+1} + \frac{([\text{D}]_{w,total} + [\text{L}]_{w,total})(P_i + (B-1)P_0)}{B})$, parameter $Y = (Bk_D P_0 \frac{[\text{H}^+]}{K_a} - P_i) (\frac{C_D k_D}{k_D+1} + \frac{C_L k_L}{k_L+1} \frac{([\text{D}]_{w,total} + [\text{L}]_{w,total})(P_i + (B-1)P_0)}{B})$ for D-NPA and parameter $Y = (Bk_L P_0 \frac{[\text{H}^+]}{K_a} - P_i) (\frac{C_D k_D}{k_D+1} + \frac{C_L k_L}{k_L+1} \frac{([\text{D}]_{w,total} + [\text{L}]_{w,total})(P_i + (B-1)P_0)}{B})$ for L-NPA. As shown in Figure 4, the plot of parameter Y versus parameter X for D-NPA yields a straight line and the slope of the line was used to evaluate K_D as 4.46 (dimensionless quantity). Similar data treatment according to eq. 22 can be performed to evaluate K_L as 18.90. The intrinsic selectivity $\alpha_{int} (K_L / K_D)$ is estimated as 4.24.

Screening of Metal Precursors

$\text{PdCl}_2(\text{CH}_3\text{CN})_2$, $[(\text{CH}_3\text{CN})_4\text{Cu}]\text{PF}_6$, $[(\text{C}_6\text{H}_5)_3\text{P}]_2\text{NiCl}_2$ were applied as the metal precursors for synthesis of chiral extractant.

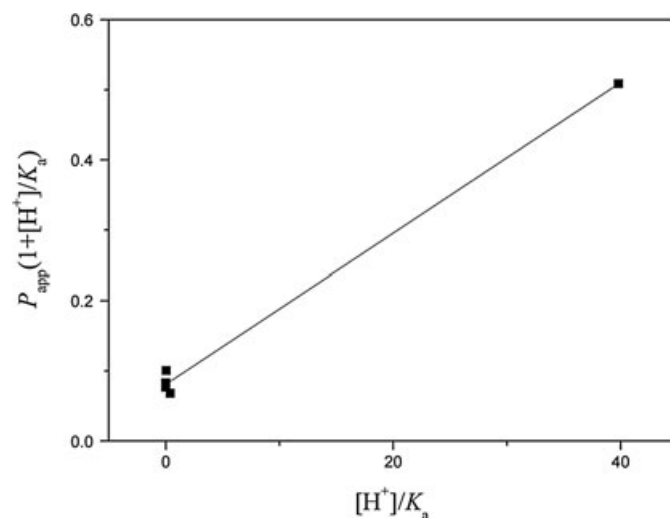


Fig. 3. Plot for calculating physical distribution coefficients P_0 and P_i for NPA in 1,2-dichloroethane-water two phase system at 5 °C. $R^2 = 0.9938$.

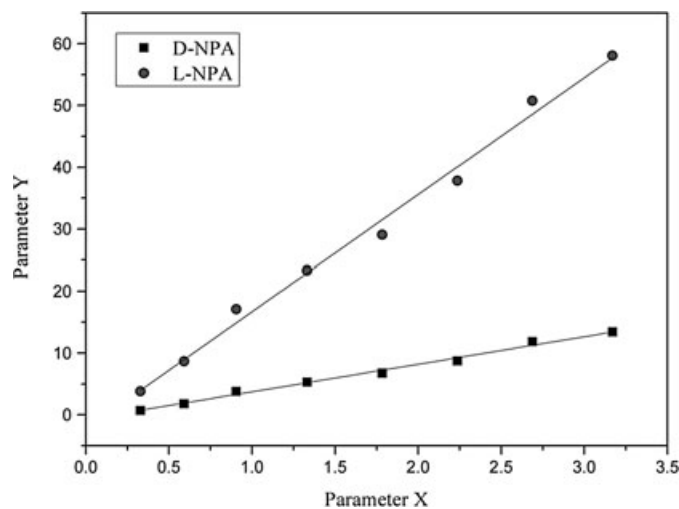


Fig. 4. Plot of calculating complexation equilibrium constants for NPA enantiomers in 1,2-dichloroethane at 5 °C. Parameter X is $P_i(C_{CuB} - \frac{C_D k_D}{k_D + 1} - \frac{C_L k_L}{k_L + 1} + \frac{([D]_{w, total} + [L]_{w, total})(P_i + (B-1)P_0)}{B})$; Parameter Y is $(Bk_D - P_0 \frac{[H^+]}{K_a} - P_i)(\frac{C_D k_D}{k_D + 1} + \frac{C_L k_L}{k_L + 1} - \frac{([D]_{w, total} + [L]_{w, total})(P_i + (B-1)P_0)}{B})$ for D-NPA and $(Bk_L - P_0 \frac{[H^+]}{K_a} - P_i)(\frac{C_D k_D}{k_D + 1} + \frac{C_L k_L}{k_L + 1} - \frac{([D]_{w, total} + [L]_{w, total})(P_i + (B-1)P_0)}{B})$ for L-NPA; $R^2 = 0.9948$ for D-NPA and $R^2 = 0.9961$ for L-NPA.

Distribution ratios (k_D and k_L) and operational selectivity (α_{op}) with different metal precursors are shown in Table 1. The highest selectivity of 2.24 is achieved using $[(CH_3CN)_4Cu]PF_6$ as metal precursor and the distribution ratios are 0.37 and 0.83, respectively. BINAP-Pd complex used as a chiral selector has been previously investigated by Verkuil et al. and a series of amino acid enantiomers were separated with good enantioselectivity.²⁸ Comparing this work with Verkuil et al.'s work, BINAP-Cu can provide a higher enantioselectivity and replacing expensive Pd with cheap Cu will be economically more interesting. The Ni-(S)-BINAP complex does not show any selectivity towards NPA enantiomers. It is obvious that copper (I) is the most suitable central ion for the chiral extractant.

Screening of Organic Solvents

The effect of organic solvents was explored using BINAP-Cu complex dissolved in different solvents. The distribution ratios and operational selectivity are shown in Table 2. It can be seen from Table 2 that organic solvent has a clear influence on the extraction performance. Good performance was obtained using the organic solvents studied. Highest enantioselectivity is obtained with 1,2-dichloroethane as organic solvents and the distribution ratios are also satisfactory. Therefore, 1,2-dichloroethane was chosen as the suitable solvent for extraction of NPA enantiomers.

TABLE 1. Influence of metal precursor

Metal precursor	k_D	k_L	α_{op}
$PdCl_2(CH_3CN)_2$	0.85	1.09	1.28
$Cu(CH_3CN)_4PF_6$	0.37	0.83	2.24
$Ni(DEEP)Cl_2$	0.13	0.13	1

Condition: $[NPA]_0 = 2.0$ mmol/L; $pH = 7.5$; $T = 5$ °C; $[(S)\text{-BINAP}]_0 = 1.0$ mmol/L; $[\text{metal precursor}]_0 = 1.0$ mmol/L; organic solvent = dichloromethane.

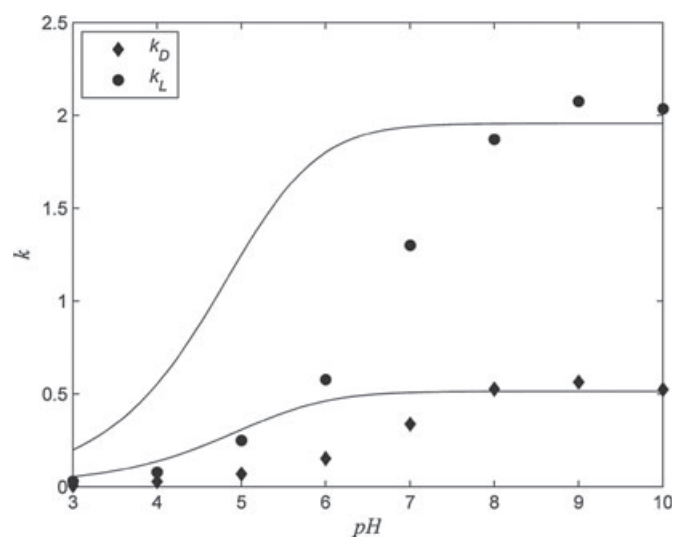
TABLE 2. Influence of organic solvent type

Organic solvent	k_D	k_L	α_{op}
1,2-dichloroethane	0.38	1.41	3.71
trichloromethane	0.91	1.64	1.80
dichloromethane	0.37	0.83	2.24
chlorobenzene	0.20	0.56	2.80

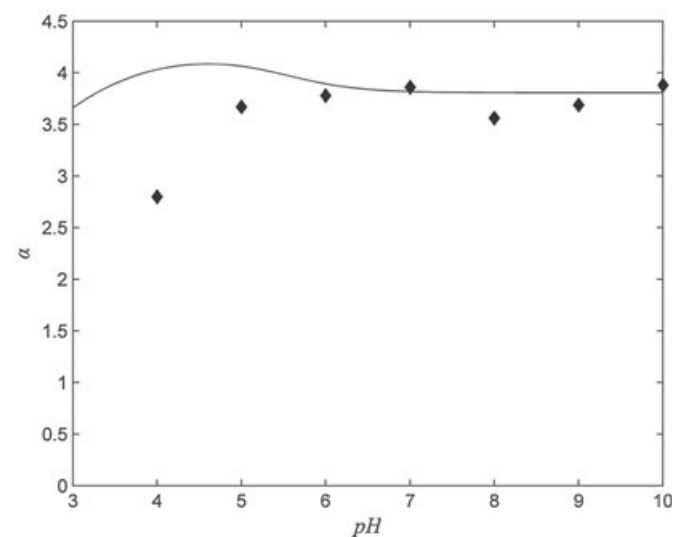
Condition: $[NPA]_0 = 2.0$ mmol/L; $pH = 7.5$; $T = 5$ °C; $[\text{BINAP-Cu}]_0 = 1.0$ mmol/L.

Influence of pH

The effect of pH of the aqueous phase on the distribution ratios and operational selectivity were investigated. We applied the interfacial reaction model to predict the distribution ratios and enantioselectivity as a function of pH. The comparison of the model predictions with the experimental results is depicted in Figure 5. It is obvious that the experimental



(a)



(b)

Fig. 5. Influence of pH on distribution ratios (a) and operational enantioselectivity (b). Solid lines: model predictions. Symbols: experimental data. Condition: solvent: 1,2-dichloroethane; $[NPA]_0 = 2.0$ mmol/L; $T = 5$ °C; $[\text{BINAP-Cu}]_0 = 1.0$ mmol/L.

values are in a good agreement with the model prediction when pH is higher than 7.

It is shown in Figure 5 that at pH below 4, distribution ratios (k_D and k_L) increase slightly with the rising of pH but k_D and k_L increase rapidly with pH rising from 5 to 7. When pH is above 7, k_D and k_L remain basically unchanged. It also can be seen that the operational enantioselectivity (α_{op}) increases with pH rising from 3 to 5; when pH rising from 5 to 6, α_{op} decreases slightly; when pH is higher than 6, α_{op} keep nearly constant. This might be explained by the fact that only NPA anion binds to the BINAP-Cu. When pH is rising, more NPA in its anion state distributes in the organic phase and is recognized by the extractant. Therefore, the distribution ratios and enantioselectivity increases. Model predictions and experimental results show a maximum α_{op} near pH of 5.

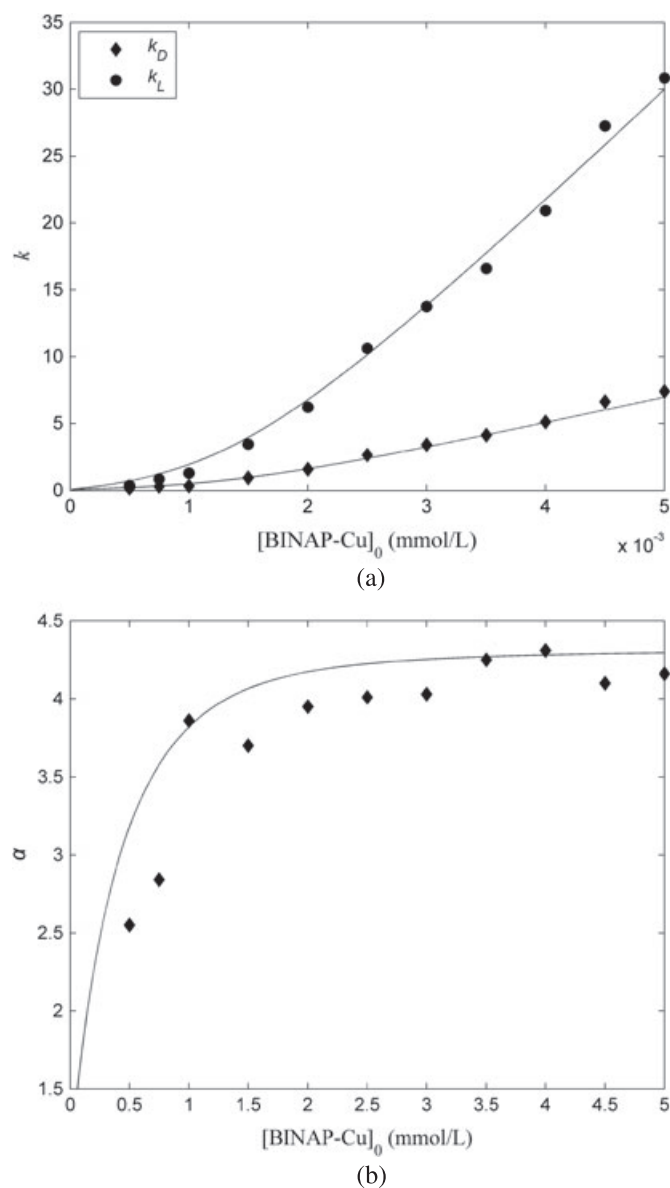


Fig. 6. Influence of host concentration on distribution ratios (a) and operational enantioselectivity (b). Solid lines: model predictions. Symbols: experimental data. Condition: solvent: 1,2-dichloroethane; [NPA]₀ = 2.0 mmol/L; T = 5 °C; pH = 7.0.

Chirality DOI 10.1002/chir

Influence of the Host Concentration

Model prediction of distribution ratios and operational selectivity is presented as solid lines, and the comparison of the experimental values with the model predictions are shown in Figure 6. It is observed that the model predicts the distribution ratios and operational selectivity accurately.

It is can be seen from Figure 6 that the distribution ratios and the operational enantioselectivity both increase with the increase of the host (BINAP-Cu) concentration, and α_{op} increases rapidly at first and then only slightly. More enantiomer–host complexes are formed in organic phase and the distribution ratios increase consequently when the host concentration increases. Meanwhile, BINAP-Cu is able to recognize enantiomers and a relatively higher concentration will enhance the recognition ability. Because of the physical partition of NPA, the correlation between host concentration and operational enantioselectivity differs from that reported by Verkuijl et al.²⁸

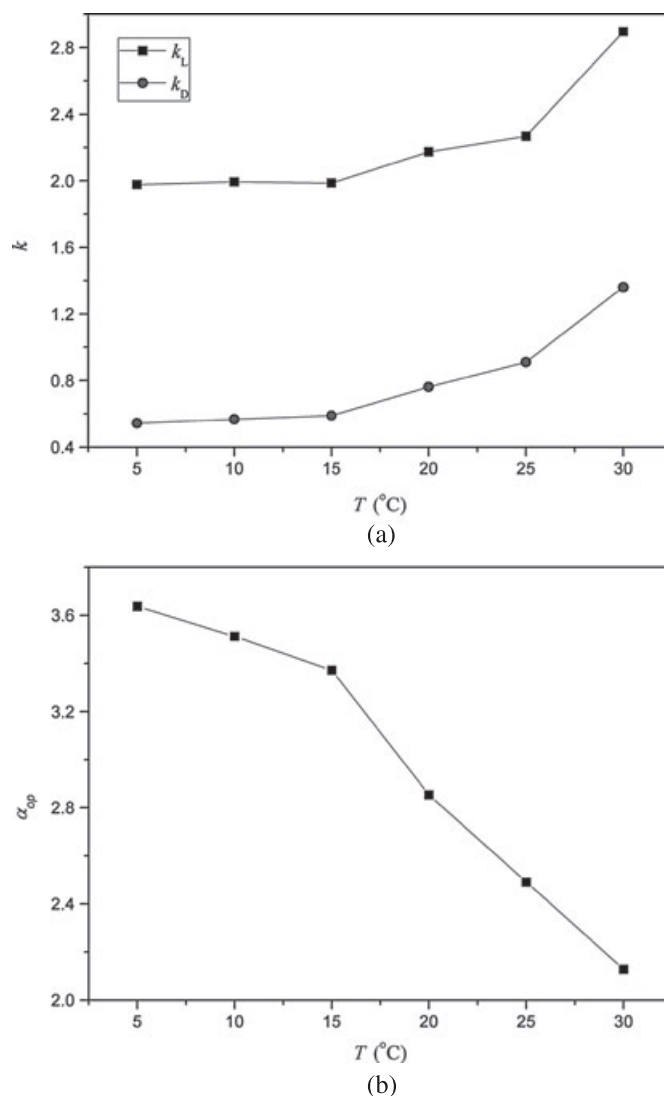


Fig. 7. Influence of temperature on distribution ratios (a) and operational enantioselectivity (b). Condition: solvent: 1,2-dichloroethane; [NPA]₀ = 2.0 mmol/L; pH = 7.0; [BINAP-Cu]₀ = 1.0 mmol/L.

Influence of Temperature

The influence of temperature on the operational enantioselectivity and distribution ratios was investigated in the range of 5–30 °C. It is seen from Figure 7 that temperature shows a strong influence on the distribution ratios and operational enantioselectivity. An increase of k_D and k_L and a decrease of α_{op} were caused by increasing temperature. However, with a temperature lower than 5 °C, the increase in viscosity of solution and the decrease of the solubility of host and substrate would make the extraction very difficult to carry out. Hence, $T=5\text{ }^\circ\text{C}$ is considered the optimal temperature for enantioselective extraction.

Modeling and Optimization

The experimental results are compared graphically with model predictions, which indicate the interfacial reaction model is a good means of predicting enantiomers partitioning over a range of process variables. Therefore, the model was used to explore the influence of various operating conditions

on extraction performance in a single stage extraction system and to optimize the operational conditions.

In Figure 8, distribution ratios and enantioselectivity of NPA enantiomers is calculated as a function of pH and host concentration, respectively. It can be found that k_D and k_L have a similar tendency with the change of pH and host concentration. The increase of pH and host concentration can give rise to distribution ratios. Enantioselectivity is strongly influenced by pH and host concentration. Maximum enantioselectivity is found at a pH of about 5 and BINAP-Cu concentration of higher than 1 mmol/L.

In Figure 9, the ee for NPA enantiomers is calculated as a function of pH and host concentration. The ee is strongly influenced by pH and the host concentration. Maximum ee (higher than 0.5) was obtained near pH = 4.0. It also illustrates that the ee increases with the increase of host concentration rapidly at first and then slightly. It is found from Figures 8 and 9 that good selectivity (α_{op}) and good purity (ee) are obtained at relatively low distribution ratios which are not conducive to increasing yield. Acquiring a good purity and a

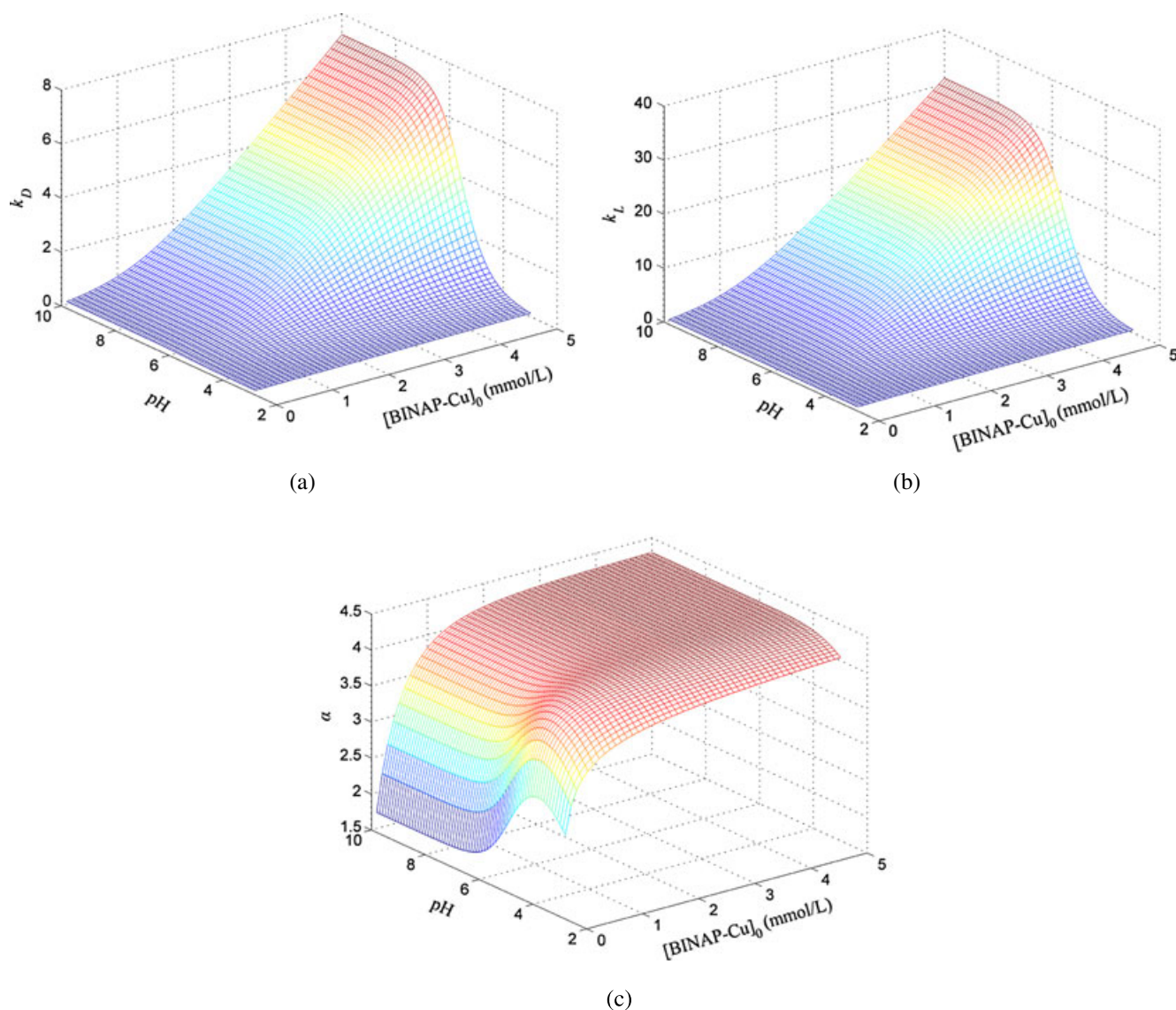


Fig. 8. Calculated distribution ratios (a, b) and enantioselectivity (c) of NPA enantiomers as a function of pH and host concentration. Condition: solvent: 1,2-dichloroethane; $[\text{NPA}]_0 = 2.0\text{ mmol/L}$; $T = 5\text{ }^\circ\text{C}$.

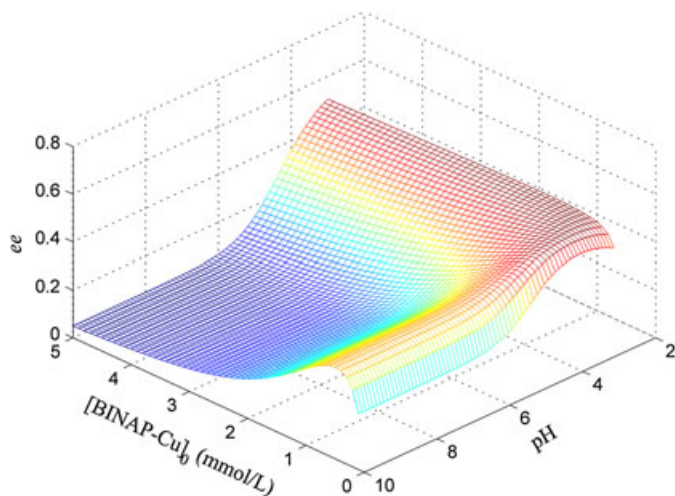


Fig. 9. Calculated enantiomeric excess (ee) for NPA enantiomers as a function of pH and host concentration. Condition: solvent: 1,2-dichloroethane; $[NPA]_0 = 2.0$ mmol/L; $T = 5^\circ\text{C}$.

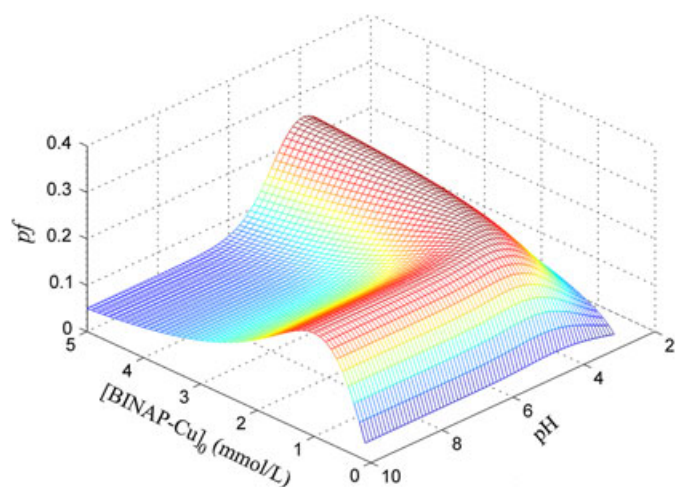


Fig. 10. Calculated performance factor (pf) for NPA enantiomers as a function of pH and host concentration. Condition: solvent: 1,2-dichloroethane; $[NPA]_0 = 2.0$ mmol/L; $T = 5^\circ\text{C}$.

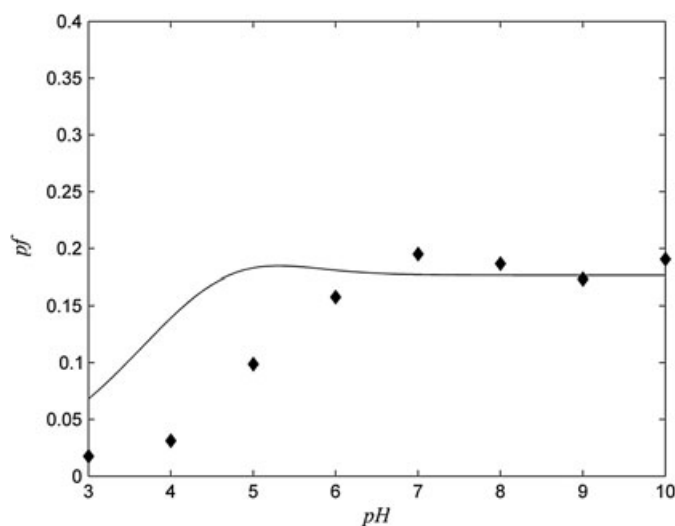


Fig. 11. Performance factor as a function of pH. Solid lines: model predictions. Symbols: experimental data. Conditions: solvent: 1,2-dichloroethane; $[NPA]_0 = 2.0$ mmol/L; $[BINAP-Cu]_0 = 1.0$ mmol/L; $T = 5^\circ\text{C}$.

Chirality DOI 10.1002/chir

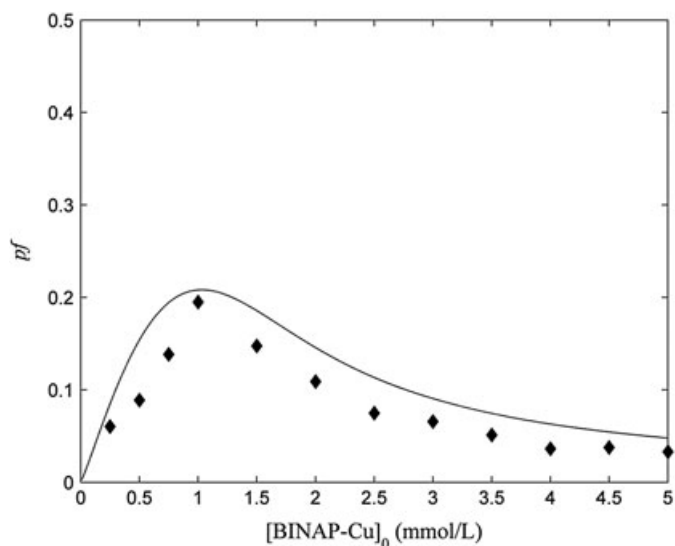


Fig. 12. Performance factor as a function of host concentration. Solid lines: model predictions. Symbols: experimental data. Conditions: solvent: 1,2-dichloroethane; $[NPA]_0 = 2.0$ mmol/L; $\text{pH} = 7.0$; $T = 5^\circ\text{C}$.

good yield are somehow contradictory. A performance factor (pf) is introduced for further optimization of the reactive extraction system.

The performance factor (pf) is defined as the product of ee in the organic phase and the fraction of enantiomer extracted into the organic phase. The given enantiomer can be purified to high purity with maximum yield in the condition with a high performance factor. Figure 10 shows the performance factors as a function of pH and host concentration. The host concentration and pH have a strong influence on the performance factor. With host concentration ranging from 1 to 2 mmol/L and pH higher than 5, a relatively high performance factor is obtained.

Performance factors were determined experimentally to support the model predictions (Figs. 11 and 12). As is shown in Figure 11, the measured performance factor increases with pH rising from 3 to 5, then decreases slightly and finally remains nearly constant at pH higher than 6. In Figure 12, the result illustrates that the performance factor increases rapidly and reaches a maximum with the increase of host concentration, and then decreases smoothly. It is observed in Figures 11 and 12 that the measured performance factor in good agreement with the model prediction. These results therefore verify the accuracy of the model and show the possibility of application for system optimization.

CONCLUSIONS

The ELLE of NPA enantiomers with metal-BINAP complex as chiral extractant (host) was investigated by experiment and modeling. Excellent agreement between the experimental data and the model predictions was observed, which indicated that the interfacial reaction model is capable of predicting the distribution of NPA enantiomers in the extraction system studied. The best conditions identified involve the use of copper(I)-BINAP complex concentration of 1 mmol/L and pH value of 7 at 5°C . Full separation of the NPA enantiomers can be achieved by multistage extraction.

LITERATURE CITED

1. Federsel HJ. Facing chirality in the 21st century: Approaching the challenges in the pharmaceutical industry. *Chirality* 2003;15:S128-S142.
2. Tombo GMR, Bellus D. Chirality and crop protection. *Angew Chem Int Ed* 1991;30:1193-1215.
3. Rouhi AM. Chiral business. *Chem Eng News* 2003;81:45-55.
4. Vries T, Wynberg H, van Echten E, Koek J, ten Hoeve W, Kellogg RM, Broxterman QB, Minnaard A, Kaptein B, van der Sluis S, Hulshof L, Kooistra J. The family approach to the resolution of racemates. *Angew Chem Int Ed* 1998;37:2349-2354.
5. Schulte M, Strube J. Preparative enantioseparation by simulated moving bed chromatography. *J Chromatogr A* 2001;906:5824-5828.
6. Zhou SY, Zuo H, Stobaugh JF, Lunte CE, Lunte SM. Continuous in vivo monitoring of amino acid neurotransmitters by microdialysis sampling with online derivatization and capillary electrophoresis separation. *Anal Chem* 1995;67:594-599.
7. Schuur B, Floure J, Hallett AJ, Winkelman JGM, de Vries JG, Heeres HJ. Continuous chiral separation of amino acid derivatives by enantioselective liquid-liquid extraction in centrifugal contactor separators. *Org Process Res Dev* 2008;12:950-955.
8. Schuur B, Winkelman JGM, Heeres HJ. Equilibrium studies on enantioselective liquid-liquid amino acid extraction using a cinchona alkaloid extractant. *Ind Eng Chem Res* 2008;47:10027-10033.
9. Prelog M, Kovacevic M, Egli M. Lipophilic tartaric acid esters as enantioselective ionophores. *Angew Chem Int Ed Engl* 1989;28:1147-1152.
10. Viegas RMC, Afonso CAM, Crespo JG, Coelho IM. Modelling of the enantio-selective extraction of propranolol in a biphasic system. *Sep Purif Technol* 2007;53:224-234.
11. Tan B, Luo GS, Wang JD. Extractive separation of amino acid enantiomers with co-extractants of tartaric acid derivative and aliquat-336. *Sep Purif Technol* 2007;53:330-336.
12. Pietraszkiewicz M, Kozbia M, Pietraszkiewicz O. Chiral discrimination of amino acids and their potassium or sodium salts by optically active crown ether derived from D-mannose. *J Membr Sci* 1998;138:109-113.
13. Steensma M, Kuipers NJM, de Haan AB, Kwant G. Influence of process parameters on extraction equilibria for the chiral separation of amines and amino-alcohols with a chiral crown ether. *J Chem Technol Biotechnol* 2006;81:588-597.
14. Colera M, Costero AM, Gaviña P, Gil S. Synthesis of chiral 18-crown-6-ethers containing lipophilic chains and their enantiomeric recognition of chiral ammonium picrates. *Tetrahedron: Asymmetry* 2005;16:2673-2679.
15. Hallett AJ, Kwant GJ, de Vries JG. Continuous separation of racemic 3,5-dinitrobenzoyl-amino acids in a centrifugal contact separator with the aid of cinchona-based chiral host compounds. *Chem Eur J* 2009;15:2111-2120.
16. Tang K, Zhang P, Pan C, Li H. Equilibrium studies on enantioselective extraction of oxybutynin enantiomers by hydrophilic β -cyclodextrin derivatives. *AIChE J* 2011;57:3027-3036.
17. Valle EMMD. Cyclodextrins and their uses: A review. *Process Biochem* 2002;38:373-377.
18. Tang K, Zhang P, Li H. Experimental and model study on the multiple chemical equilibrium for reactive extraction of ibuprofen enantiomers with HP- β -CD as hydrophilic selector. *Process Biochem* 2011;46:1817-1824.
19. Tang K, Yi J, Huang K, Zhang G. Biphasic recognition chiral extraction: A novel method for separation of mandelic acid enantiomers. *Chirality* 2009;21:390-395.
20. Koska J, Haynes CA. Modeling multiple chemical equilibria in partition systems. *Chem Eng Sci* 2001;56:5853-5864.
21. Dimitrova P, Bart HJ. Extraction of amino acid enantiomers with microemulsions. *Chem Eng Technol* 2009;32:1527-1534.
22. Tang L, Choi S, Nandhakumar R, Park H, Chung H, Chin J, Kim KM. Reactive extraction of enantiomers of 1,2-amino alcohols via stereoselective thermodynamic and kinetic processes. *J Org Chem* 2008;73:5996-5999.
23. Yoon J, Cram DJ. Chiral recognition properties in complexation of two asymmetric hemiacetals. *J Am Chem Soc* 1997;119:11796-11806.
24. Ding HB, Carr PW, Cussler EL. Racemic leucine separation by hollow-fiber extraction. *AIChE J* 1998;38:1493-1498.
25. Snyder SE, Carey JR, Pirkle WH. Biphasic enantioselective partitioning studies using small-molecule chiral selectors. *Tetrahedron* 2005;61:7562-7567.
26. Steensma M, Kuipers NJM, de Haan AB, Kwant G. Identification of enantioselective extractants for chiral separation of amines and amino alcohols. *Chirality* 2006;18:314-328.
27. Kocabas E, Karakucuk A, Sirit A, Yilmaz M. Synthesis of new chiral calyx [4]arene diamide derivatives for liquid phase extraction of α -amino acid methyl esters. *Tetrahedron: Asymmetry* 2006;17:1514-1520.
28. Verkuijl BJV, Minnaard AJ, de Vries JG, Feringa BL. Chiral separation of underivatized amino acids by reactive extraction with palladium-BINAP complexes. *J Org Chem* 2009;74:6526-6533.
29. Verkuijl BJV, Schuur B, Minnaard AJ, de Vries JG, Feringa BL. Chiral separation of substituted phenylalanine analogues using chiral palladium phosphine complexes with enantioselective liquid-liquid extraction. *Org Biomol Chem* 2010;8:3045-3054.
30. Foster AC, Li Y, Staubli U, Viswanath V, Luhrs L. D-serine transporter inhibitors as pharmaceutical compositions for the treatment of central nervous system disorders. U.S. Patent: 20,120,329,851. 2012.